

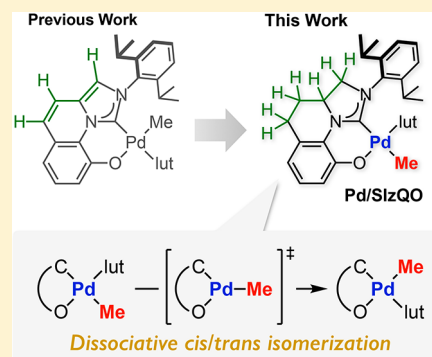
Synthesis and Reactivity of Methylpalladium Complexes Bearing a Partially Saturated IzQO Ligand

Shumpei Akita, Ryo Nakano, Shingo Ito,[†] and Kyoko Nozaki*[†]

Department of Chemistry and Biotechnology, Graduate School of Engineering, The University of Tokyo, 7-3-1 Hongo, Bunkyo-ku, Tokyo 113-8656, Japan

Supporting Information

ABSTRACT: A saturated N-heterocyclic carbene–phenolate bidentate ligand, 3,3a,4,5-tetrahydroimidazo[1,5-*a*]quinolin-9-olate-1-ylidene (SIzQO), was synthesized and characterized. The SIzQO ligand was then treated with PdClMe(pyridine)₂ and [Pd(μ -Cl)Me(2,6-lutidine)]₂, which afforded *C,C*-*cis*-(SIzQO)PdMe(pyridine) and the thermodynamically unstable *trans* isomer *C,C*-*trans*-(SIzQO)PdMe(2,6-lutidine), respectively. The latter isomerizes at 40 °C into the corresponding *cis* isomer via a dissociative mechanism. These palladium/SIzQO complexes catalyze the polymerization of ethylene at 100–120 °C, although the catalytic activity is lower than that of a previously reported palladium/imidazo[1,5-*a*]quinolin-9-olate-1-ylidene (IzQO) system.



INTRODUCTION

In the last two decades, coordination–insertion copolymerization of olefins with polar monomers has been investigated as a means to introduce functional groups into polyolefins such as polyethylene and polypropylene.¹ For that purpose, group 10 metals, which tend to exhibit relatively high tolerance toward polar functional groups, are the catalysts of choice owing to their “soft” nature: i.e., their low oxophilicity.¹ The most representative catalysts for such copolymerizations are palladium/phosphine–sulfonate catalysts (**1**; Figure 1), which were initially reported by Drent et al. in 2002² and since then have been intensively studied by many other researchers.^{1b,d,3} In these studies, successful copolymerizations

have been attributed to the use of bidentate ligands that bear a strong σ -donor (e.g., phosphine) and a weak σ -donor (e.g., sulfonate), which enables the formation of linear polyethylenes with high molecular weight by suppression of β -hydride elimination as side reactions.⁴ This design is also effective for the development of many other types of bidentate phosphine ligands bearing a weak σ -donor.^{5–7}

Apart from phosphines, N-heterocyclic carbene (NHC) ligands have been applied to group 10 metal catalyzed copolymerization reactions as strong σ -donors (Figure 1).⁸ Although the initially reported catalysts, including **2**^{8c} and **3**,^{8a} exhibited low catalytic activity, presumably owing to catalyst decomposition,⁸ we have recently developed an imidazo[1,5-*a*]quinolin-9-olate-1-ylidene (IzQO) ligand (**4**), whose palladium complexes were successfully applied to ethylene and propylene/polar monomer copolymerization reactions.⁹ The role of the rigid backbone of the IzQO ligand lies in preventing the rotation of the NHC plane toward the palladium plane so that reductive elimination leading to catalyst decomposition is suppressed effectively. In this context, we hypothesized that the introduction of a saturated NHC group, which should have σ -donating properties stronger than those of an unsaturated NHC,¹⁰ should further enhance the activity toward polar monomer copolymerization via destabilization of the σ -coordination of polar monomers on the metal center. Here, we report the synthesis and characterization of palladium complexes **5**, which bear a partially saturated IzQO ligand, i.e., 3,3a,4,5-tetrahydroimidazo[1,5-*a*]quinolin-9-olate-1-ylidene (SIzQO), as well as their activity in the polymerization of

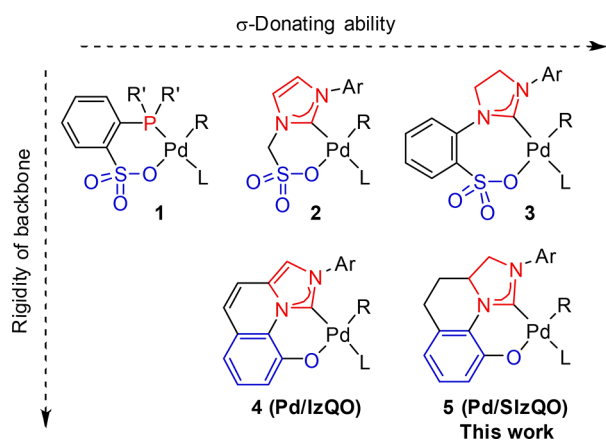


Figure 1. Palladium complexes with unsymmetric bidentate ligands used for the polymerization of olefins.

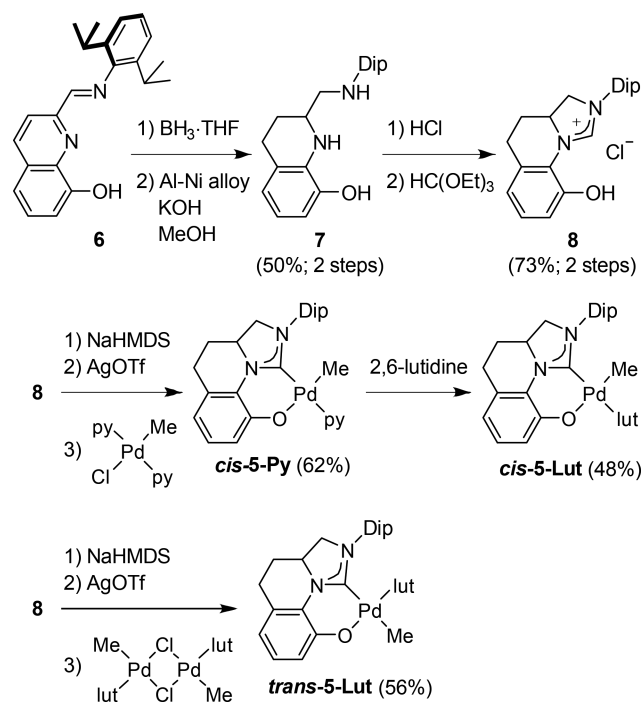
Received: April 25, 2018

ethylene. During our investigations, we were able to isolate a thermodynamically unstable *C,C-trans* isomer, which revealed an unprecedented *trans/cis* isomerization behavior.

RESULTS AND DISCUSSION

Preparation of the SIzQO Ligand and Its Palladium Complexes. The synthetic route to ligand precursor **8** is shown in Scheme 1. Starting from **6**,¹¹ the imine moiety was

Scheme 1. Synthesis of SIzQO Precursor **8 and Its Palladium Complexes **5****



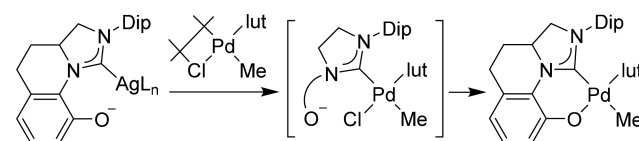
reduced with $\text{BH}_3\cdot\text{THF}$ and, subsequently, the quinoline backbone was partially hydrogenated in the presence of Al-Ni alloy to afford diimine **7** in two-step 50% yield. Diamine **7** was protonated with hydrogen chloride and treated with excess triethyl orthoformate to afford imidazolium salt **8**. After recrystallization from dichloromethane/hexane, pure **8** was obtained in 73% yield in two steps from **7**.

In order to prepare Pd/SIzQO complexes, **8** was deprotonated with NaHMDS and treated with AgOTf. The obtained Ag/SIzQO intermediate was then treated with $\text{PdClMe}(\text{pyridine})_2$ or $[\text{Pd}(\mu\text{-Cl})\text{Me}(2,6\text{-lutidine})_2]$, which afforded the corresponding Pd/SIzQO complexes. Notably, the obtained *cis/trans* structure depended on the palladium precursor: when *trans*- $\text{PdClMe}(\text{pyridine})_2$ was used, *C,C-cis* complex *cis*-**5-Py**, in which the carbene ligand and methyl group are located *cis* to each other, was obtained in 62% yield. In contrast, a reaction of the Ag/SIzQO intermediate with $[\text{Pd}(\mu\text{-Cl})\text{Me}(2,6\text{-lutidine})_2]$ furnished *C,C-trans* complex *trans*-**5-Lut** in 56% yield. The *C,C-trans* isomer should be thermodynamically less stable than the *cis* isomer, as the carbene ligand and the methyl group, both of which exhibit a strong *trans* influence, are located *trans* to each other. Complex *cis*-**5-Lut** was synthesized by a ligand exchange reaction from *cis*-**5-Py** in 48% yield.

Possible Mechanism for the Formation of the *C,C-trans* Isomer. A possible mechanism for the formation of

trans-**5-Lut** is shown in Scheme 2. In general, ligand substitution occurs more easily at a position *trans* to a ligand

Scheme 2. Possible Mechanism for the Formation of *trans*-5-Lut** from the Reaction of Silver/SIzQO and $[\text{Pd}(\mu\text{-Cl})\text{Me}(2,6\text{-lutidine})_2]$**



with a stronger *trans* effect. The *trans* effect of carbenes and methyl groups is stronger than that of 2,6-lutidine, pyridine, and phenolate.¹⁰ When $[\text{Pd}(\mu\text{-Cl})\text{Me}(2,6\text{-lutidine})_2]$ is used as the methylpalladium precursor, the NHC initially coordinates to the palladium center via dissociation of the chlorido group *trans* to the methyl group.¹² Subsequently, the other chlorido group is replaced by the aryloxy moiety of the SIzQO ligand, which affords *trans*-**5-Lut**. If the aryloxy moiety coordinates to palladium more quickly than NHC, it would provide *cis*-**5-Lut** (see Section 5 in the Supporting Information for the detailed mechanistic explanation). However, ¹H NMR analysis revealed no contamination of *cis*-**5-Lut** in the crude product.

X-ray Diffraction Analysis of Pd/SIzQO Complexes.

The solid-state structures of *cis*-**5-Py**, *cis*-**5-Lut**, and *trans*-**5-Lut** were confirmed by single-crystal X-ray diffraction analyses (Figure 2 and Table 1). A comparison of the bond lengths of Pd/SIzQO complexes **5** and Pd/IzQO complex **4** revealed that the Pd–N3 bond length of *cis*-**5-Lut** (2.136(4) Å) is significantly longer than that in *cis*-**4-Lut** (2.095(2) Å). This discrepancy may be attributed to the fact that the σ -donating properties of saturated NHCs are stronger than those of unsaturated NHCs.¹⁰ The Pd–N3 bond length is significantly shorter in *cis*-**5-Py** (2.095(2) Å) than in *cis*-**5-Lut** (2.136 Å), which may be due to the steric congestion involving the methyl groups of 2,6-lutidine. A similar trend has been observed in bis(*o*-methoxyphenyl)phosphine–sulfonate-supported palladium complexes (2.108(3) Å vs 2.134(2) Å).¹³ Subsequently, we examined the lengths of the Pd–Me bonds for the three *C,C-cis* Pd/SIzQO complexes, which were almost identical (*cis*-**5-Py**, 2.050(3) Å; *cis*-**5-Lut**, 2.055(5) Å; *cis*-**4-Lut**, 2.060(6) Å). We also observed that the C2–Pd1–N3 angle in *trans*-**5-Lut** (100.85(14)°) is larger than the C2–Pd1–C1 angle in *cis*-**5-Py** (94.47(12)°). This difference should be due to the steric repulsion between the Dip substituent and 2,6-lutidine in *trans*-**5-Lut**. The same trend has been reported for the *cis/trans* isomers of **3** (89.1(4) and 100.14(12) Å, respectively).^{8d}

In a previous paper on Pd/IzQO catalysts, we proposed that the mean dihedral angle between the NHC plane and the palladium coordination plane should be correlated to the stability of the metal catalysts during polymerization reactions.^{9a} The calculated dihedral angle is 34.2° in *cis*-**5-Lut** and 34.6° in *trans*-**5-Lut**.^{8f} The dihedral angles of the Pd/SIzQO complexes **5-Lut** are higher than that of the Pd/IzQO complex *cis*-**4-Lut** (22.3°, see Section 3 in the Supporting Information for comparison) and comparable to those of ethylene polymerization catalysts such as a Ni/IzQO complex (33.1°)^{9b} and a Pd/carbene–phosphine oxide complex (32.5°).^{8f}

Polymerization of Ethylene. Ethylene polymerization reactions were performed with *cis*-**5-Lut** at 100 °C (Table 2,

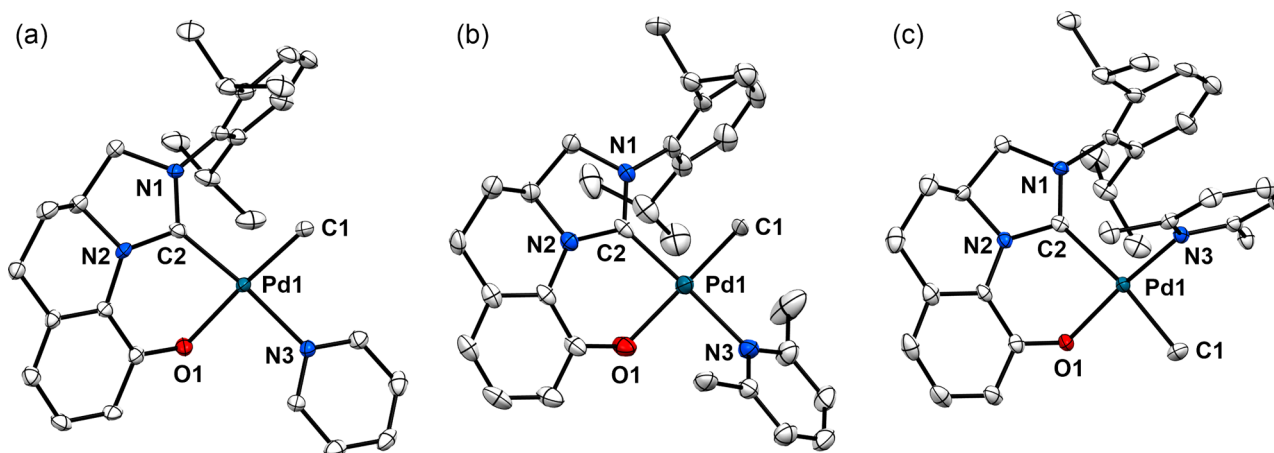


Figure 2. Single-crystal X-ray structures of (a) *cis*-5-Py, (b) *cis*-5-Lut, and (c) *trans*-5-Lut with thermal ellipsoids set to 50% probability. Hydrogen atoms and solvent molecules are omitted for clarity, and only selected atoms have been labeled.

Table 1. Representative Bond Lengths (Å) and Angles (deg) in Palladium Complexes 4 and 5

	<i>cis</i> -5-Py	<i>cis</i> -5-Lut	<i>trans</i> -5-Lut	<i>cis</i> -4-Lut ^{9a}
Pd1–C1	2.050(3)	2.055(5)	2.060(4)	2.060(6)
Pd1–C2	1.961(3)	1.953(5)	2.091(4)	1.965(7)
Pd1–N3	2.095(2)	2.136(4)	2.046(3)	2.095(6)
Pd1–O1	2.085(2)	2.096(3)	2.037(3)	2.062(4)
C2–Pd1–O1	88.63(10)	87.49(16)	84.74(13)	89.7(2)
C1–Pd1–C2	94.47(12)	92.68(18)	173.13(16)	97.0(3)
C1–Pd1–N3	90.39(11)	90.23(17)	85.52(16)	89.3(3)
C2–Pd1–N3	175.01(10)	176.52(17)	100.85(14)	173.2(3)
dihedral angle (NHC/Pd)	29.5	34.2	34.6	22.3
dihedral angle (Pd/pyridine)	49.5	77.3	75.2	82.7

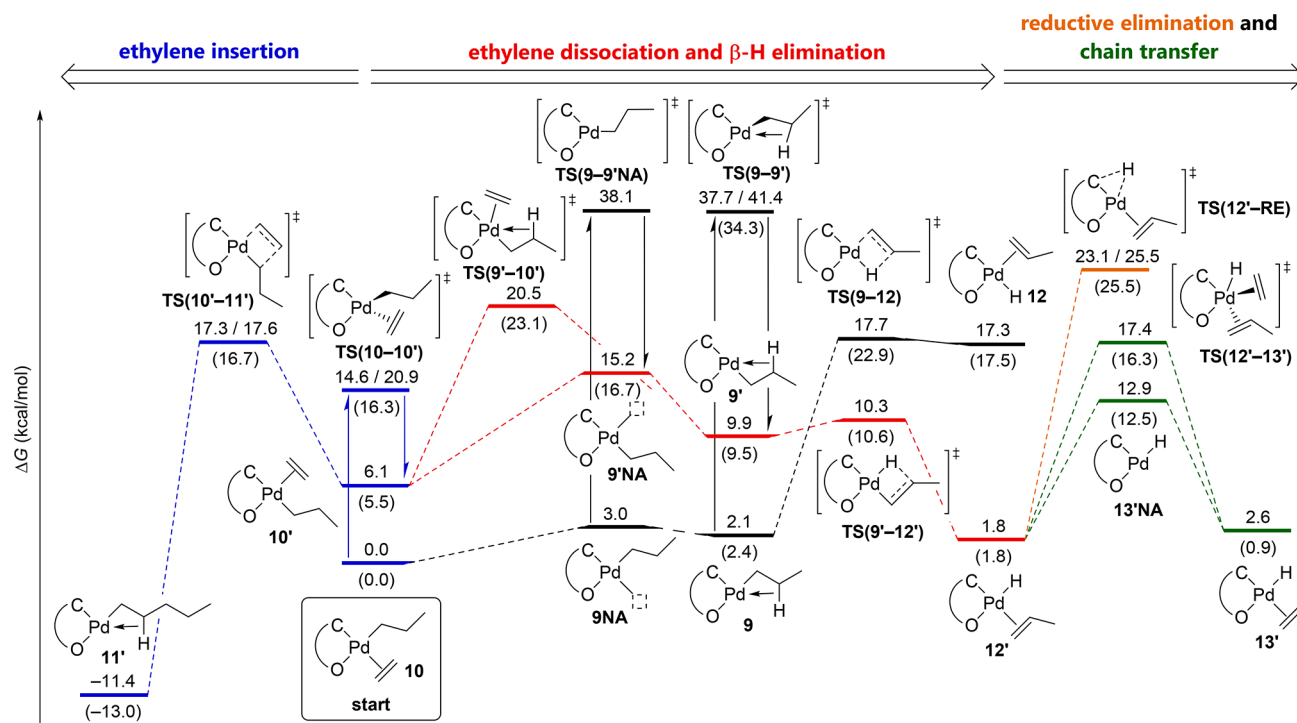
entry 1), which resulted in an activity of 3.6 kg mol⁻¹ h⁻¹ and the formation of polyethylene with a number-averaged molecular weight (M_n) of 1.8 × 10³. The polymerization activity of *cis*-5-Lut is more than 100 times lower than that of *cis*-4-Lut (entries 1 and 6), and the M_n value of the resulting polyethylene is more than 10 times lower than that obtained with *cis*-4-Lut. The methyl branches in the polymer chains

obtained from using *cis*-5-Lut accounted for 33.3 per 1000 carbons, a value which is higher than that using *cis*-4-Lut (11.6). These results suggest that the rate of the β -hydride elimination and the subsequent chain transfer or branch formation becomes relatively fast in comparison to that with Pd/IzQO complex 4. We also attempted the polymerization of ethylene using *cis*-5-Py in order to investigate the effect of the fourth ligand; however, the results obtained were comparable (entry 2). In the case of *trans*-5-Lut (entries 3–6), the observed polymerization activity was also comparable (entry 3). The reaction after 2.0 h (entry 4) afforded an increased amount of polyethylene in comparison to that after 1.0 h (entry 3). We also probed the effect of polymerization temperature (entries 5 and 6). While *trans*-5-Lut did not afford any polyethylene at 80 °C, the formation of a black precipitate on the polymer was observed after polymerization at 120 °C (entry 6). The observed polymerization activities of catalysts 5 (3.6–5.3 kg mol⁻¹ h⁻¹) are lower than those of typical group 10 metal catalysts such as palladium/ α -diimine (20–8800 kg mol⁻¹ h⁻¹)^{1h,14} and palladium/phosphine-sulfonate (120–5330 kg mol⁻¹ h⁻¹)^{4a} catalysts. The above experimental results suggested lower stabilities of 5 in

Table 2. Polymerization of Ethylene using Pd/SIzQO Catalysts 4 and 5^a

entry	cat. (amt (μmol))	temp (°C)	time (h)	activity (kg mol ⁻¹ h ⁻¹)	10 ³ M_n ^b	M_w/M_n	branches/1000C ^c
1 ^d	<i>cis</i> -5-Lut (10)	100	1.0	3.6	1.8	3.6	33.3
2 ^d	<i>cis</i> -5-Py (10)	100	1.0	5.2	2.5	2.0	28.9
3 ^d	<i>trans</i> -5-Lut (10)	100	1.0	5.3	7.0	1.7	28.2
4 ^d		100	2.0	4.1	3.6	3.1	27.6
5 ^d		80	1.0	trace			
6 ^d		120	1.0	4.7	3.9	2.4	34.2
7 ^d	<i>cis</i> -4-Lut (1.0)	100	1.0	691	76.0	2.1	11.6

^aA mixture of the catalyst (10 μmol) and ethylene (4.0 MPa at 20 °C) in toluene (20 mL) was stirred for 1.0 h at the indicated temperature. ^bNumber-average molecular weight measured by SEC using internal polystyrene standards and corrected by universal calibration. ^cNumber of methyl branches determined by quantitative ¹³C NMR analysis. ^dData from ref 9a.

Scheme 3. Energy Profile of the Ethylene-Insertion and β -Hydride-Elimination Pathways Using Pd/SzQO Complex 5^a

^aValues in parentheses refer to Pd/IzQO complex 4.

comparison to 4, which prompted us to investigate the mechanism by the density functional theory (DFT) method.

DFT Calculations on the Ethylene Polymerization Mechanism. In order to clarify the reasons behind the low activity of the SzQO systems, DFT calculations were performed with the B3LYP functional¹⁵ with empirical dispersion correction, DFT-D3,¹⁶ the LanL2DZ basis set¹⁷ and effective core potential for palladium, and the 6-31G(d) basis sets¹⁸ for the light atoms. To include solvation effects (with toluene as the solvent), the SMD solvation model¹⁹ was employed.

Initially, we investigated the pathway for the insertion of ethylene (Scheme 3). The insertion of ethylene using group 10 metal catalysts with an unsymmetrical bidentate ligand proceeds via ethylene coordination, *cis/trans* isomerization, and the insertion of ethylene (blue). Considering intermediate 10 as the starting complex, the transition states of the Pd/SzQO systems for the *cis/trans* isomerization TS(10-10') were calculated to be at 14.6 and 20.9 kcal/mol, respectively, depending on the rotational direction. It should be noted that the SzQO ligand contains chiral centers in its backbone; therefore, two diastereotopic transition states should be considered in some cases. The difference in ΔG values for TS(10-10') of the Pd/SzQO system is 6.3 kcal/mol. The transition states for the insertion of ethylene TS(10'-11') were calculated to be 17.3 and 17.6 kcal/mol, which are slightly higher than those of the Pd/IzQO catalyst (*cis/trans* isomerization, 16.3 kcal/mol; insertion of ethylene, 16.7 kcal/mol).

The differences in molecular weight of the polymers obtained from 4 and 5 may be explained by the differences in the β -hydride-elimination pathway (red). In the Pd/SzQO system, the transition state for the β -hydride elimination TS(9'-12') obtained from *trans*-alkyl species 9' (10.3 kcal/mol)

is lower than that of TS(9-12), which originates from *cis*-alkyl species 9 (17.7 kcal/mol); therefore, the latter is not considered in the following discussion. Of the possible pathways to generate intermediate 9', we considered the dissociation of ethylene from 10' via either the three-coordinated intermediate 9'NA (15.2 kcal/mol) or five-coordinated intermediate TS(9'-10') (20.5 kcal/mol). The difference between 9'NA and TS(9'-10') by 5.3 kcal/mol may not be significant considering the presence of a high excess amount of ethylene under the polymerization conditions.^{4a} In the literature, the mole fraction of ethylene in toluene at 90 °C under 3.8 MPa of ethylene was reported to be 0.24, meaning that 60 mmol of ethylene is present in 190 mmol (=20 mL at 20 °C) of toluene under the conditions.²⁰ Since we charged 4.0 MPa of ethylene at 20 °C (and heated the closed system to 80–120 °C) for polymerization, it can be reasonably assumed that >6000 equiv of ethylene to the palladium catalyst 5 (10 μ mol) exists in the liquid phase under the reaction conditions. The pathway 9 \rightarrow TS(9-9') \rightarrow 9' was ruled out because TS(9-9') is much higher in energy than 9'NA and TS(9'-10'). Overall, the β -hydride-elimination route 10' \rightarrow 9'NA \rightarrow 9' \rightarrow TS(9'-12') \rightarrow 12' (15.2 kcal/mol) is ≥ 2.1 kcal/mol lower in energy than the ethylene-insertion pathway 10' \rightarrow TS(10'-11') \rightarrow 11' (17.3/17.6 kcal/mol). In the case of Pd/IzQO complex 4, the ΔG value of 9'NA (16.7 kcal/mol) is identical with that of TS(10'-11') (16.7 kcal/mol). These results are thus consistent with the experimental data, in which Pd/SzQO complexes 5 afforded polymers with lower molecular weights and higher numbers of branches in comparison to those obtained from Pd/IzQO complex 4.

We also elucidated the fate of the hydride complex 12'. Chain termination may occur via reductive elimination of C and H (brown) or chain transfer reactions (green). The

contribution of the former reductive elimination pathway may be limited due to its high activation energy (23.1/25.5 kcal/mol) (see Section 6.1 in the Supporting Information for the details). For the chain transfer reactions, the dissociation pathway $12' \rightarrow 13'_{\text{NA}} \rightarrow 13'$ (12.9 kcal/mol) is energetically more favorable than the association pathway $12' \rightarrow \text{TS}(12' - 13') \rightarrow 13'$ (17.4 kcal/mol). These values are comparable to those obtained using a previously reported Pd/IzQO catalyst (12.5 and 16.3 kcal/mol, respectively).

On the basis of the DFT study on complexes **4** and **5**, the lower stability and higher branch-forming rate of **5** in comparison to those of **4** during ethylene polymerization are reasoned as follows. The rate of the key steps for ethylene polymerization, namely *cis/trans* isomerization and ethylene insertion, were found to be comparable between the two catalysts. However, the ethylene dissociation steps, $9'_{\text{NA}}$ and $\text{TS}(9' - 10')$, leading to β -hydride elimination are faster in the case of complex **5**. This could be attributed to the stronger electron donation provided by the saturated NHC moiety of **5**, which stabilizes low-coordinated electron-poor species such as $9'$ and $9'_{\text{NA}}$. Clearly, the branch formation and catalyst decomposition happen after β -hydride elimination. It should also be noted that the catalyst decomposition via C–H reductive elimination, $\text{TS}(12' - \text{RE})$, is faster in complex **5** than in complex **4**. Structurally, this can be explained by the greater twisting of the saturated NHC plane from the metal square (Table 1), increasing the crucial orbital overlapping for C–H reductive elimination between the vacant p-orbital on the carbene carbon and the σ -orbital of the *cis*-Pd–hydride bond. Electronically, the saturated NHCs are better π -acceptor than the unsaturated NHCs, implying more susceptibility for nucleophilic attack of the hydride onto the vacant p-orbital of the carbene carbon (see Section 6.2 in the Supporting Information for the details).²¹

Isomerization Reaction of *trans*-5-Lut. One of the key steps in the catalytic polymerization of ethylene using group 10 metal complexes with unsymmetric bidentate ligands is *cis/trans* isomerization. It is therefore not surprising that the *cis/trans* isomerization of square-planar d^8 -metal complexes of e.g. Pd(II) has been studied intensely.²² Our mechanistic studies on palladium/phosphine–sulfonate systems by DFT calculations revealed that the *cis/trans* isomerization of palladium/phosphine–sulfonate complexes proceeds via a transition state which is similar to that in Berry's pseudorotation mechanism (Scheme 4a).^{4a} Jordan and co-workers have reported in their studies on *cis/trans* isomerization of palladium/phosphine–sulfonate complexes that the Berry's pseudorotation mechanism is assisted by either the sulfonate group or an additional lutidine molecule (Scheme 4b).²³ For carbene–sulfonate complex **3**, the isomerization was proposed to proceed via a dissociation of the sulfonate group (Scheme 4c),^{8d} which was based on the fact that the isomerization was not affected by the addition of lutidine but rather was influenced by the addition of a Lewis acid such as $\text{B}(\text{C}_6\text{F}_5)_3$. Mapolie and co-workers have experimentally confirmed that platinum/imine–phenolate complex **6** isomerizes via a tetrahedral intermediate (Scheme 4d), although DFT calculations suggested that a dissociative pathway should be energetically comparable.²⁴

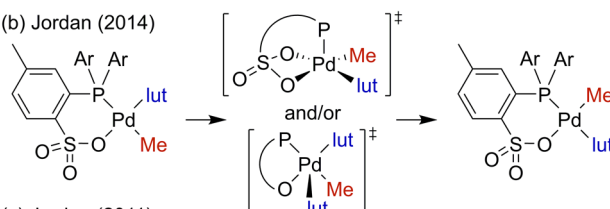
Against this background, we investigated the isomerization behavior of *trans*-5-Lut into *cis* isomer *cis*-5-Lut. A solution of *trans*-5-Lut (10 μmol) in CH_2Cl_2 (0.50 mL) was heated to 40 °C and monitored by ^1H NMR spectroscopy using 1,2,4,5-tetrabromobenzene as the internal standard (Scheme 5). After

Scheme 4. Proposed Mechanisms for the Isomerization of Group 10 Metal Complexes with a Bidentate Ligand

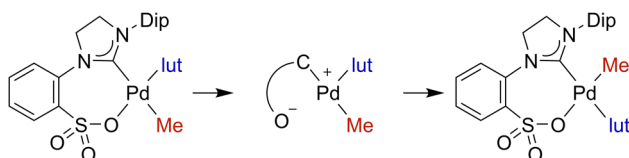
(a) Nozaki (2009, 2016)



(b) Jordan (2014)



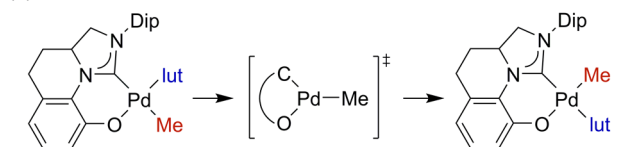
(c) Jordan (2011)



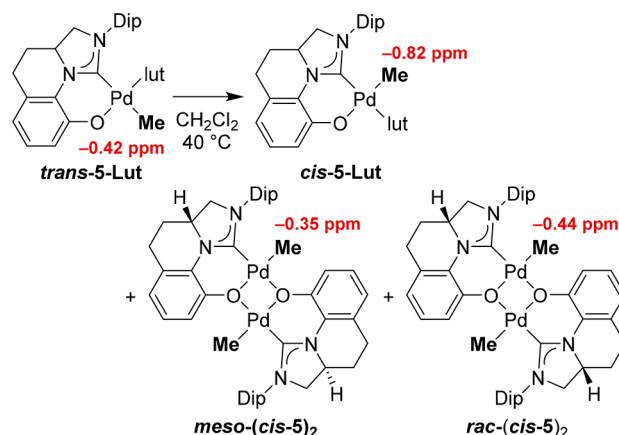
(d) Mapolie (2013)



(e) This Work



Scheme 5. *cis/trans* Isomerization of *trans*-5-Lut



12 h, 40% of *trans*-5-Lut had been consumed and three new singlet resonances, attributable to the methyl groups, appeared in the negative region of the ^1H NMR spectrum (−0.35, −0.44, and −0.82 ppm). The species at −0.82 ppm was assigned to *cis*-5-Lut by comparison with an authentic sample.²⁵ In order to confirm the structures of the other two species, a solution of the crude reaction mixture was layered with pentane and stored at −35 °C to obtain colorless single crystals. The ^1H NMR spectrum of the crystals in CD_2Cl_2 showed a singlet resonance at −0.44 ppm, and an X-ray

diffraction analysis revealed the crystals to be *rac*-(*cis*-5)₂ (Figure 3). Consequently, the signal at −0.35 ppm was

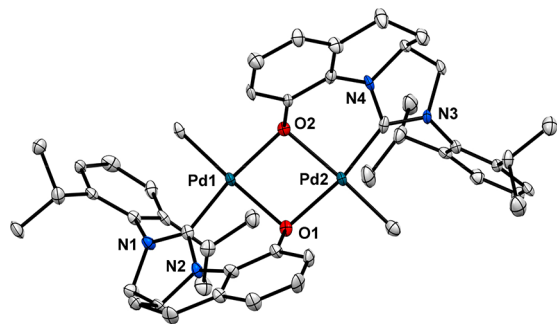


Figure 3. Single-crystal X-ray structure of *rac*-(*cis*-5)₂ with thermal ellipsoids set to 50% probability. Hydrogen atoms are omitted for clarity, and only selected atoms have been labeled. Selected bond lengths (Å) and angles (deg): Pd1–O1 = 2.155(5), Pd1–O2 = 2.105(5), Pd2–O1 = 2.132(5), Pd2–O2 = 2.170(5), Pd1–Pd2 = 3.1818(14); C2–Pd1–O1 = 88.3(3), O1–Pd1–O2 = 88.3(3).

associated with *meso*-(*cis*-5)₂. Note that *cis*-5-Lut, *rac*-(*cis*-5)₂, and *meso*-(*cis*-5)₂ are confirmed to be in equilibrium on the basis of the following observations. ¹H NMR analysis of the isolated *cis*-5-Lut revealed the presence of *cis*-5-Lut and *rac*- and *meso*-(*cis*-5)₂ in CD₂Cl₂ solution, and the addition of extra 2,6-lutidine cleanly afforded a mixture of pure *cis*-5-Lut and free 2,6-lutidine.

The time course of the isomerization (Figure 4) revealed that the conversion of *trans*-5-Lut stopped after 3 h. This

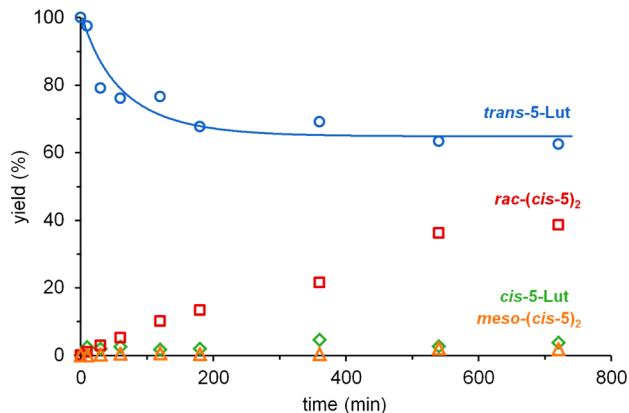


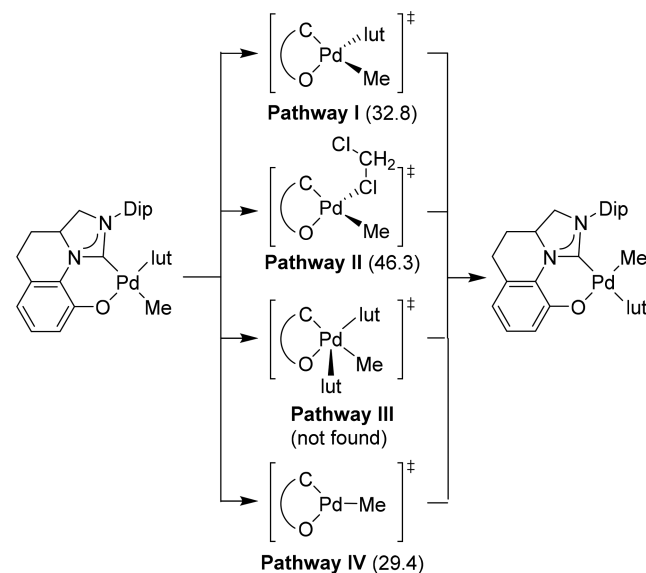
Figure 4. Time course plot of the isomerization reaction of *trans*-5-Lut at 40 °C.

phenomenon could be rationalized in terms of an equilibrium between *trans*-5 and *cis*-5; however, this possibility was dismissed, as the attempted isomerization of *cis*-5-Lut did not proceed and as DFT calculations suggested that *trans*-5-Lut should be 8.2 kcal/mol more stable than *cis*-5-Lut. Another possibility is that a byproduct generated during the isomerization could suppress the isomerization. Assuming that 2,6-lutidine quenches the isomerization, we investigated the reaction of *trans*-5-Lut in the presence of 1.5 equiv of 2,6-lutidine. Indeed, we observed that the isomerization was suppressed and that *trans*-5-Lut decomposed instead (see Section 5 in the Supporting Information for the details).

On the basis of the aforementioned background, four possible mechanisms for the isomerization of *trans*-5-Lut into

cis-5-Lut can be considered (Scheme 6). One corresponds to the isomerization via a tetrahedrally coordinated intermediate

Scheme 6. Possible Mechanisms for the Isomerization of Pd/SIzQO Complexes



through coordination of either 2,6-lutidine (pathway I) or solvent (CH₂Cl₂) (pathway II); however, pathway I can be dismissed, as it would not be affected by the addition of 2,6-lutidine. Another possible mechanism is the isomerization via Berry's pseudorotation (pathway III), which would be accelerated upon addition of 2,6-lutidine. Thus, pathway III is not probable in this case either. Our experimental results that the presence of additional lutidine suppressed the *cis/trans* isomerization suggest that only pathways II and IV are possible (Table 3).

Table 3. Summary of Experimental and Computational Studies on the Mechanism of *cis/trans* Isomerization of Complex 5-Lut

	pathway			
	I	II	III	IV
experiment	×	✓	×	✓
calculation	✓	×	×	✓
activation energy(kcal/mol)	32.8	46.3	not found	29.4

Next, DFT calculations were carried out (see Sections 6.3 and 6.4 in the Supporting Information for the details). We could identify the transition states for pathways I, II, and IV, while a five-coordinated TS in pathway III could not be found. The estimated activation energy of dissociative pathway IV (29.4 kcal/mol) and that of pathway I via the tetrahedral transition state (32.8 kcal/mol) are much lower than that of pathway II involving solvent coordination (46.3 kcal/mol). Considering the experimental and theoretical results in their entirety, we conclude that the dissociative pathway (pathway IV) is operative in this reaction (Table 3).

CONCLUSION

In summary, Pd/SIzQO complexes **5** were synthesized, characterized, and employed as catalysts in the polymerization

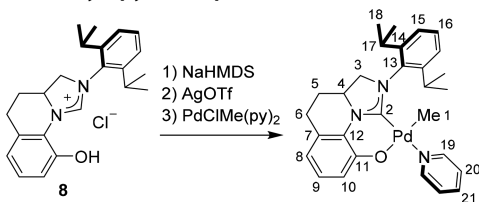
of ethylene. The catalytic activity of **5** was more than 100 times lower than that of the corresponding Pd/IzQO catalyst (**4**). During the investigation of the Pd/SizQO system, an unstable *C,C-trans* isomer, *trans-5-Lut*, was isolated and characterized. Complex *trans-5-Lut* isomerized at 40 °C into *cis* isomers *cis-5-Lut* and (*cis-5*)₂. The isomerization proceeds via the dissociation of 2,6-lutidine, which is supported by the results of experimental and theoretical investigations.

EXPERIMENTAL SECTION

General Procedures of Ethylene Polymerization. A 50 mL stainless steel autoclave was dried in an oven at 120 °C, sealed, and evacuated under vacuum until it cooled to room temperature. In the autoclave charged with argon were placed catalyst (10 μmol) and anhydrous toluene (20 mL). Then, the autoclave was pressurized with ethylene (4.0 MPa) and the contents were stirred in an isothermal heating block for 1.0 h at given temperature. After redundant ethylene was vented, the reaction was quenched by addition of methanol (ca. 50 mL). The formed precipitates were collected by filtration, washed with methanol, and dried under high vacuum at 100 °C for at least for 5 h to afford polyethylene. The molecular weights and their distribution were determined by size exclusion chromatography. The extent of branching in the polymer backbone was determined by quantitative ¹³C NMR spectroscopy.

General Procedures of *cis/trans* Isomerization of *trans-5-Lut* in the Presence and Absence of 2,6-Lutidine. An NMR tube was charged with *trans-5-Lut* (5.8 mg, 10 μmol) and 1,2,4,5-tetrabromobenzene (1.0 mg) under an argon atmosphere. To the mixture was added CH₂Cl₂ (0.50 mL) or a solution of 2,6-lutidine in CH₂Cl₂ (30 mM, 0.50 mL). The NMR tube was kept at a given temperature and monitored by ¹H NMR spectroscopy. The conversion of *trans-5-Lut* and the amounts of products were determined by integration of Pd–CH₃ resonances relative to 1,2,4,5-tetrabromobenzene (δ 7.90 ppm in CD₂Cl₂, 7.89 ppm in CH₂Cl₂) as an internal standard. Since the signals of Pd–CH₃ in *rac-(cis-5)*₂ and *trans-5-Lut* were overlapped, the two signals were separated by wave separation method (see Section 5 in the Supporting Information for the details). A crystal of *rac-(cis-5)*₂ appropriate for X-ray crystallographic analysis was prepared as follows. After the isomerization, the solution was layered with an excess amount of hexane. After storage at –35 °C overnight, *rac-(cis-5)*₂ was obtained as white crystals.

Preparation of *cis-5-Py*: (SP-4-4)-[2-(2,6-Diisopropylphenyl)-3,3a,4,5-tetrahydroimidazo[1,5-*a*]quinolin-9-olato-κO-1-ylidene-κC¹](methyl)(pyridine)palladium.



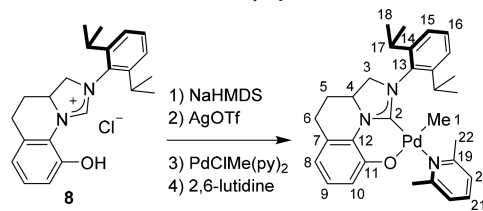
To a mixture of 8-hydroxy-2-(2,6-diisopropylphenyl)imidazolino[1,5-*a*]quinolinium chloride (**8**; 38.5 mg, 0.10 mmol) and sodium bis(trimethylsilyl)amide (NaHMDS; 36.8 mg, 0.10 mmol) in a 15 mL vial was added benzene (5.0 mL). After the mixture was stirred for 15 min at room temperature, silver triflate (28.2 mg, 0.11 mmol) was added. After the mixture was stirred for 30 min, PdClMe(pyridine)₂ (31.5 mg, 0.10 mmol) was added. The mixture was stirred for 1.0 h at room temperature. The mixture was filtered through a pad of Celite, and the filtrate was evaporated to dryness. The formed solid was dissolved in a minimum amount of THF with 1 drop of pyridine and layered with an excess amount of pentane. After storage at –35 °C overnight, the title compound was obtained as yellow crystals (34.0 mg, 62% yield).

Note: ¹H NMR spectroscopic analysis revealed that *cis-5-Py* is in equilibrium with the dimeric species (*cis-5*)₂. ¹H and ¹³C NMR

spectra were recorded in the presence of additional pyridine in order not to form (*cis-5*)₂.

¹H NMR (500 MHz, CD₂Cl₂): δ ca. 8.6 (2H, H19, overlapped with those of free pyridine), 7.76 (t, ³J_{HH} = 7.6 Hz, 1H, H21), 7.37 (t, ³J_{HH} = 7.8 Hz, 1H, H16), 7.33 (t, ³J_{HH} = 6.9 Hz, 2H, H20), ca. 7.30 (1H, H15, overlapped with those of free pyridine), 7.17 (dd, ³J_{HH} = 7.9 Hz, ⁴J_{HH} = 1.5 Hz, 1H, H15), 6.83 (dd, ³J_{HH} = 7.6, 7.6 Hz, 1H, H9), 6.57 (dd, ³J_{HH} = 7.9 Hz, ⁴J_{HH} = 0.9 Hz, 1H, H8), 6.28 (dd, ³J_{HH} = 7.3 Hz, ⁴J_{HH} = 0.9 Hz, 1H, H10), 4.26–4.20 (m, 1H, H4), 3.92 (dd, ²J_{HH} = 10.8 Hz, ³J_{HH} = 10.8 Hz, 1H, H3), 3.76 (dd, ²J_{HH} = 10.7 Hz, ³J_{HH} = 6.1 Hz, 1H, H3), 3.49 (1H, sept, ³J_{HH} = 6.7 Hz, 1H, H17), 3.18 (sept, ³J_{HH} = 6.7 Hz, 1H, H17), 3.06 (m, 1H, H6), 2.96 (dd, ²J_{HH} = 17.1 Hz, ³J_{HH} = 5.5 Hz, 1H, H6), 2.18–2.05 (m, 2H, H5), 1.75 (d, ³J_{HH} = 6.7 Hz, 3H, H18), 1.35 (d, ³J_{HH} = 7.0 Hz, 3H, H18), 1.28 (t, ³J_{HH} = 6.1 Hz, 3H, H18), 1.21 (d, ³J_{HH} = 6.7 Hz, 3H, H18), –0.59 (s, 3H, H1). ¹³C{¹H} NMR (126 MHz, CD₂Cl₂): δ 192.1 (C, C2), 161.1 (1C, C11), 150.5 (2C, C19), 147.0 (1C, C14), 146.5 (1C, C14), 137.4 (1C, C21), 136.7 (1C, C13), 129.5 (1C, C12), 128.5 (1C, C16), 127.4 (1C, C7), 125.1 (1C, C9), 124.7 (2C, C20), 124.4 (1C, C15), 123.7 (1C, C15), 116.1 (1C, C8), 112.5 (1C, C10), 59.8 (1C, C3), 57.8 (1C, C4), 30.1 (1C, C5), 28.5 (1C, C17), 28.4 (1C, C17), 26.8 (1C, C6), 25.8 (1C, C18), 25.7 (1C, C18), 24.3 (1C, C18), 23.4 (1C, C18), –10.0 (1C, C1). HRMS (ESI): *m/z* calcd for C₂₉H₃₆N₃OPd⁺ ([M + H]⁺) 548.1893, found 548.1897.

Preparation of *cis-5-Lut*: (SP-4-4)-[2-(2,6-Diisopropylphenyl)-3,3a,4,5-tetrahydroimidazo[1,5-*a*]quinolin-9-olato-κO-1-ylidene-κC¹](2,6-lutidine)(methyl)palladium.



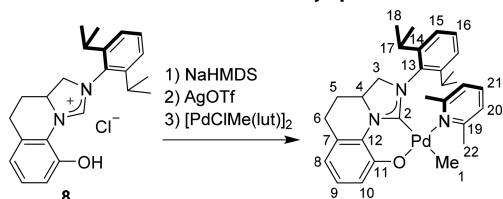
To a mixture of 8-hydroxy-2-(2,6-diisopropylphenyl)imidazolino[1,5-*a*]quinolinium chloride (**8**; 76.9 mg, 0.20 mmol) and sodium bis(trimethylsilyl)amide (NaHMDS; 73.3 mg, 0.20 mmol) in a 15 mL vial was added benzene (10.0 mL). After the mixture was stirred for 15 min at room temperature, silver triflate (56.5 mg, 0.22 mmol) was added. After the mixture was stirred for 30 min, PdClMe(pyridine)₂ (63.0 mg, 0.20 mmol) was added. The mixture was stirred for 1.0 h at room temperature. The mixture was filtered through a pad of Celite, and the filtrate was evaporated to dryness. The crude product of the complex *cis-5-Py* was dissolved in THF (ca. 5.0 mL), and to the solution was added 2,6-lutidine (ca. 1.0 mL). The solution was shaken for several minutes, and the volatile materials were removed under vacuum. This procedure was repeated twice to remove residual pyridine. The obtained solid was dissolved in a minimum amount of THF with 1 drop of lutidine and layered with an excess amount of pentane. After storage at –35 °C overnight, the title compound was obtained as yellow crystals (55.0 mg, 48% yield).

Note: ¹H NMR spectroscopic analysis revealed that *cis-5-Lut* is in equilibrium with the dimeric species (*cis-5*)₂. ¹H and ¹³C NMR spectra were recorded in the presence of additional 2,6-lutidine in order not to form (*cis-5*)₂.

¹H NMR (500 MHz, CD₂Cl₂): δ 7.50 (t, ³J_{HH} = 7.7 Hz, 1H, H21), 7.35 (t, ³J_{HH} = 7.7 Hz, 1H, H16), 7.28 (dd, ³J_{HH} = 7.8 Hz, ⁴J_{HH} = 1.4 Hz, 1H, H15), 7.16 (dd, ³J_{HH} = 7.6 Hz, ⁴J_{HH} = 1.5 Hz, 1H, H15), 7.02 (d, ³J_{HH} = 7.6 Hz, 2H, H20), 6.74 (dd, ³J_{HH} = 7.8, 7.8 Hz, 1H, H9), 6.33 (d, ³J_{HH} = 8.1 Hz, 1H, H10), 6.23 (d, ³J_{HH} = 7.0 Hz, 1H, H8), 4.26–4.19 (m, 1H, H4), 4.02 (dd, ²J_{HH} = 10.8 Hz, ³J_{HH} = 10.8 Hz, 1H, H3), 3.79 (sept, ³J_{HH} = 6.8 Hz, 1H, H17), 3.71 (dd, ²J_{HH} = 10.7 Hz, ³J_{HH} = 7.3 Hz, 1H, H3), 3.15 (sept, ³J_{HH} = 6.9 Hz, 1H, H17), 3.09–2.95 (m, 2H, H6), 2.91 (s, 3H, H22), 2.84 (s, 3H, H22), 2.20–2.17 (m, 2H, H5), 1.61 (d, ³J_{HH} = 6.9 Hz, 3H, H18), 1.31 (d, ³J_{HH} = 6.7 Hz, 3H, H18), 1.27 (d, ³J_{HH} = 6.7 Hz, 3H, H18), 1.20 (d, ³J_{HH} = 6.9 Hz, 3H, H18), –0.82 (s, 3H, H1). ¹³C{¹H} NMR (126 MHz, CD₂Cl₂): δ 190.6 (1C, C2), 161.8 (1C, C11), 159.8 (1C, C19), 159.0

(1C, C19), 147.2 (1C, C14), 147.1 (1C, C14), 137.7 (1C, C21), 137.6 (1C, C13), 129.9 (1C, C12), 128.9 (1C, C16), 127.4 (1C, C7), 125.3 (1C, C9), 124.5 (1C, C15), 124.3 (1C, C15), 122.4 (1C, C20), 122.1 (1C, C20), 116.6 (1C, C8), 112.6 (1C, C10), 60.5 (1C, C3), 57.9 (1C, C4), 30.8 (1C, C5), 28.9 (1C, C17), 28.7 (1C, C17), 27.3 (1C, C6), 27.2 (1C, C22), 26.3 (1C, C18), 26.2 (1C, C22), 26.0 (1C, C18), 23.7 (1C, C18), 23.6 (1C, C18), -14.8 (1C, C1). HRMS (ESI): m/z calcd for $C_{31}H_{40}N_3OPd^+$ ($[M + H]^+$) 576.2201, found 576.2233.

Preparation of *trans*-5-Lut: (*SP*-4-2)-[2-(2,6-Diisopropylphenyl)-3,3a,4,5-tetrahydroimidazo[1,5-*a*]quinolin-9-olato- κ O-1-ylidene- κ C¹](2,6-lutidine)(methyl)palladium.



To a mixture of 8-hydroxy-2-(2,6-diisopropylphenyl)imidazolino[1,5-*a*]quinolinium chloride (**8**; 76.9 mg, 0.20 mmol) and sodium bis(trimethylsilyl)amide (73.3 mg, 0.40 mmol) in a 15 mL vial was added benzene (10 mL). After the mixture was stirred for 30 min at room temperature, silver triflate (56.5 mg, 0.22 mmol) was added. After the mixture was stirred for 30 min, $[Pd(\mu-Cl)Me(2,6-lutidine)]_2$ (52.8 mg, 0.10 mmol) was added. The mixture was stirred for 1.0 h. The mixture was filtered through a pad of Celite, and the filtrate was evaporated to dryness. The formed solid was dissolved in a minimum amount of THF and layered with an excess amount of pentane. After storage at $-35^\circ C$ overnight, the title compound was obtained as bright yellow crystals (64.3 mg, 56% yield). A crystal appropriate for X-ray crystallographic analysis was prepared by recrystallization from CH_2Cl_2 (containing 0.5% of methanol)/hexane bilayering at $-35^\circ C$.

1H NMR (500 MHz, CD_2Cl_2 , room temperature): δ 7.29 (t, $^3J_{HH} = 7.6$ Hz, 1H, H21), 7.26 (d, $^3J_{HH} = 5.8$ Hz, 1H, H15), 7.26 (d, $^3J_{HH} = 3.4$ Hz, 1H, H15), 6.91 (d, $^3J_{HH} = 7.6$ Hz, 1H, H20), 6.82 (dd, $^3J_{HH} = 5.8$, 3.4 Hz, 1H, H16), 6.78 (t, $^3J_{HH} = 7.8$ Hz, 1H, H9), 6.72 (d, $^3J_{HH} = 7.6$ Hz, 1H, H20), 6.60 (dd, $^3J_{HH} = 7.9$ Hz, $^4J_{HH} = 1.5$ Hz, 1H, H10), 6.35 (dd, $^3J_{HH} = 7.5$ Hz, $^4J_{HH} = 1.4$ Hz, 1H, H8), 4.28–4.21 (m, 1H, H4), 3.81 (dd, $^2J_{HH} = 10.7$ Hz, $^3J_{HH} = 10.7$ Hz, 1H, H3), 3.66 (dd, $^2J_{HH} = 10.7$ Hz, $^3J_{HH} = 8.2$ Hz, 1H, H3), 3.18 (sept, $^3J_{HH} = 6.9$ Hz, 1H, H17), 3.08–2.95 (m, 2H, H6), 2.82 (s, 3H, H22), 2.62 (sept, $^3J_{HH} = 6.9$ Hz, 1H, H17), 2.28–2.24 (m, 1H, H5), 2.21 (s, 3H, H22), 1.96 (m, 1H, H5), 1.69 (d, $^3J_{HH} = 6.7$ Hz, 3H, H18), 1.17 (d, $^3J_{HH} = 7.0$ Hz, 3H, H18), 1.03 (d, $^3J_{HH} = 6.7$ Hz, 3H, H18), 0.40 (d, $^3J_{HH} = 7.0$ Hz, 3H, H18), -0.44 (s, 3H, H1). $^{13}C\{^1H\}$ NMR (126 MHz, CD_2Cl_2 , room temperature): δ 205.5 (1C, C2), 161.7 (1C, C11), 161.2 (1C, C19), 159.6 (1C, C19), 148.4 (1C, C14), 147.1 (1C, C14), 137.5 (1C, C13), 136.5 (1C, C21), 130.9 (1C, C12), 128.9 (1C, C15), 127.1 (1C, C7), 125.2 (1C, C15), 125.0 (1C, C9), 123.6 (1C, C16), 122.0 (1C, C20), 121.8 (1C, C20), 117.6 (1C, C10), 114.0 (1C, C8), 60.4 (1C, C3), 58.7 (1C, C4), 30.6 (1C, C5), 29.0 (1C, C17), 28.3 (1C, C17), 28.1 (1C, C22), 27.5 (1C, C22), 27.4 (1C, C6), 27.0 (1C, C18), 25.8 (1C, C18), 24.3 (1C, C18), 22.1 (1C, C18), 1.9 (1C, C1). HRMS (ESI): m/z calcd for $C_{31}H_{39}N_3NaOPd^+$ ($[M + Na]^+$) 598.2026, found 598.2011. Anal. Calcd for $C_{31}H_{39}N_3OPd \cdot CH_3OH \cdot 1/2SCH_2Cl_2$: C, 61.87; H, 7.00; N, 6.72. Found: C, 61.96; H, 6.96; N, 6.71.

Computational Details. All calculations were performed using the Gaussian 09 packages.²⁶ The DFT (B3LYP-D3) methods^{15,16} chosen were used primarily with 6-31G(d) basis sets¹⁸ for the light atoms and the LanL2DZ basis sets¹⁷ and effective core potential for palladium. To include solvation effects (toluene as the solvent for the ethylene polymerization and dichloromethane as the solvent for the isomerization reaction), the SMD solvation model¹⁸ was employed.

■ ASSOCIATED CONTENT

Supporting Information

The Supporting Information is available free of charge on the ACS Publications website at DOI: 10.1021/acs.organomet.8b00263.

Experimental procedures and characterization data of ligands, palladium complexes, and polymers, X-ray crystallographic data for *cis*-5-Py, *cis*-5-Lut, *trans*-5-Lut, and (*cis*-5)₂, and details of the calculations (PDF) Computed Cartesian coordinates of all of the molecules reported in this study (XYZ)

Accession Codes

CCDC 1833823–1833826 contain the supplementary crystallographic data for this paper. These data can be obtained free of charge via www.ccdc.cam.ac.uk/data_request/cif, or by emailing data_request@ccdc.cam.ac.uk, or by contacting The Cambridge Crystallographic Data Centre, 12 Union Road, Cambridge CB2 1EZ, UK; fax: +44 1223 336033.

■ AUTHOR INFORMATION

Corresponding Author

*E-mail for K.N.: nozaki@chembio.t.u-tokyo.ac.jp.

ORCID

Shingo Ito: 0000-0003-1776-4608

Kyoko Nozaki: 0000-0002-0321-5299

Notes

The authors declare no competing financial interest.

■ ACKNOWLEDGMENTS

This work was supported by JST CREST Grant Number JPMJCR1323 (Japan). A part of this work was conducted at the Research Hub for Advanced Nano Characterization, The University of Tokyo, supported by MEXT of Japan. The theoretical calculations were performed using computational resources provided by Research Center for Computational Science, National Institutes of Natural Sciences, Okazaki, Japan. S.A. thanks the Program for Leading Graduate Schools (MERIT) from the JSPS.

■ REFERENCES

- (1) For reviews, see: (a) Ittel, S. D.; Johnson, L. K.; Brookhart, M. Late-Metal Catalysts for Ethylene Homo- and Copolymerization. *Chem. Rev.* **2000**, *100*, 1169–1203. (b) Nakamura, A.; Ito, S.; Nozaki, K. Coordination–Insertion Copolymerization of Fundamental Polar Monomers. *Chem. Rev.* **2009**, *109*, S215–S244. (c) Ito, S.; Nozaki, K. Coordination–Insertion Copolymerization of Polar Vinyl Monomers by Palladium Catalysts. *Chem. Rev.* **2010**, *10*, 315–325. (d) Nakamura, A.; Anselment, T. M. J.; Claverie, J.; Goodall, B.; Jordan, R. F.; Mecking, S.; Rieger, B.; Sen, A.; van Leeuwen, P. W. N. M.; Nozaki, K. Ortho-Phosphinobenzenesulfonate: A Superb Ligand for Palladium–Catalyzed Coordination Insertion Copolymerization of Polar Vinyl Monomers. *Chem. Res.* **2013**, *46*, 1438–1449. (e) Carrow, B. P.; Nozaki, K. Transition-Metal-Catalyzed Functional Polyolefin Synthesis: Effecting Control through Chelating Ancillary Ligand Design and Mechanistic Insights. *Macromolecules* **2014**, *47*, 2541–2555. (f) Baier, M. C.; Zuideveld, M. A.; Mecking, S. Post-Metalloenes in the Industrial Production of Polyolefins. *Angew. Chem., Int. Ed.* **2014**, *53*, 9722–9744. (g) Mu, H.; Pan, L.; Song, D.; Li, Y. Neutral Nickel Catalysts for Olefin Homo- and Copolymerization: Relationships between Catalyst Structures and Catalytic Properties. *Chem. Rev.* **2015**, *115*, 12091–12137. (h) Guo, L.; Dai, S.; Sui, X.; Chen, C. Palladium and Nickel Catalyzed Chain Walking Olefin Polymerization and Copolymerization. *ACS Catal.* **2016**, *6*,

428–441. (i) Ito, S. Chain-Growth Polymerization Enabling Formation/Introduction of Arylene Groups into Polymer Main Chains. *Polym. J.* **2016**, *48*, 667–677. (j) Ito, S. Palladium-Catalyzed Homo- and Copolymerization of Polar Monomers: Synthesis of Aliphatic and Aromatic Polymers. *Bull. Chem. Soc. Jpn.* **2018**, *91*, 251–261.

(2) Drent, E.; van Dijk, R.; van Ginkel, R.; van Oort, B.; Pugh, R. I. Palladium Catalyzed Copolymerisation of Ethene with Alkylacrylates: Polar Comonomer Built into the Linear Polymer Chain. *Chem. Commun.* **2002**, 744–745.

(3) For representative reports since 2014, see: (a) Ota, Y.; Ito, S.; Kuroda, J.; Okumura, Y.; Nozaki, K. Quantification of the Steric Influence of Alkylphosphine–Sulfonate Ligands on Polymerization, Leading to High-Molecular-Weight Copolymers of Ethylene and Polar Monomers. *J. Am. Chem. Soc.* **2014**, *136*, 11898–11901. (b) Jian, Z.; Wucher, P.; Mecking, S. Heterocycle-Substituted Phosphinesulfonato Palladium(II) Complexes for Insertion Copolymerization of Methyl Acrylate. *Organometallics* **2014**, *33*, 2879–2888. (c) Contrella, N. D.; Jordan, R. F. Lewis Acid Modification and Ethylene Oligomerization Behavior of Palladium Catalysts That Contain a Phosphine-Sulfonate-Diethyl Phosphonate Ancillary Ligand. *Organometallics* **2014**, *33*, 7199–7208. (d) Jian, Z.; Mecking, S. Insertion Homo- and Copolymerization of Diallyl Ether. *Angew. Chem., Int. Ed.* **2015**, *54*, 15845–15849. (e) Chen, M.; Yang, B.; Chen, C. Redox-Controlled Olefin (Co)Polymerization Catalyzed by Ferrocene-Bridged Phosphine-Sulfonate Palladium Complexes. *Angew. Chem., Int. Ed.* **2015**, *54*, 15520–15524. (f) Schuster, N.; Rünzi, T.; Mecking, S. Reactivity of Functionalized Vinyl Monomers in Insertion Copolymerization. *Macromolecules* **2016**, *49*, 1172–1179. (g) Jian, Z.; Leicht, H.; Mecking, S. Direct Synthesis of Imidazolium-Functional Polyethylene by Insertion Copolymerization. *Macromol. Rapid Commun.* **2016**, *37*, 934–938. (h) Wu, Z.; Chen, M.; Chen, C. Ethylene Polymerization and Copolymerization by Palladium and Nickel Catalysts Containing Naphthalene-Bridged Phosphine-Sulfonate Ligands. *Organometallics* **2016**, *35*, 1472–1479. (i) Jian, Z.; Mecking, S. Insertion Polymerization of Divinyl Formal. *Macromolecules* **2016**, *49*, 4395–4403. (j) Jian, Z.; Falivene, L.; Boffa, G.; Sánchez, S. O.; Caporaso, L.; Grassi, A.; Mecking, S. Direct Synthesis of Telechelic Polyethylene by Selective Insertion Polymerization. *Angew. Chem., Int. Ed.* **2016**, *55*, 14378–14383. (k) Wei, J.; Shen, Z.; Filatov, A. S.; Liu, Q.; Jordan, R. F. Self-Assembled Cage Structures and Ethylene Polymerization Behavior of Palladium Alkyl Complexes That Contain Phosphine-Bis(Arenesulfonate) Ligands. *Organometallics* **2016**, *35*, 3557–3568. (l) Ota, Y.; Ito, S.; Kobayashi, M.; Kitade, S.; Sakata, K.; Tayano, T.; Nozaki, K. Crystalline Isotactic Polar Polypropylene from the Palladium-Catalyzed Copolymerization of Propylene and Polar Monomers. *Angew. Chem., Int. Ed.* **2016**, *55*, 7505–7509. (m) Wada, S.; Jordan, R. F. Olefin Insertion into a Pd–F Bond: Catalyst Reactivation Following β -F Elimination in Ethylene/Vinyl Fluoride Copolymerization. *Angew. Chem., Int. Ed.* **2017**, *56*, 1820–1824. (n) Chen, M.; Chen, C. Rational Design of High-Performance Phosphine Sulfonate Nickel Catalysts for Ethylene Polymerization and Copolymerization with Polar Monomers. *ACS Catal.* **2017**, *7*, 1308–1312. (o) Yang, B.; Pang, W.; Chen, M. Redox Control in Olefin Polymerization Catalysis by Phosphine–Sulfonate Palladium and Nickel Complexes. *Eur. J. Inorg. Chem.* **2017**, *2017*, 2510–2514. (p) Liang, T.; Chen, C. Side-Arm Control in Phosphine-Sulfonate Palladium- and Nickel-Catalyzed Ethylene Polymerization and Copolymerization. *Organometallics* **2017**, *36*, 2338–2344. (q) Wu, Z.; Hong, C.; Du, H.; Pang, W.; Chen, C. Influence of Ligand Backbone Structure and Connectivity on the Properties of Phosphine-Sulfonate Pd(II)/Ni(II) Catalysts. *Polymers* **2017**, *9*, 168. (r) Black, R. E.; Jordan, R. F. Synthesis and Reactivity of Palladium(II) Alkyl Complexes That Contain Phosphine-Cyclopentanesulfonate Ligands. *Organometallics* **2017**, *36*, 3415–3428. (s) Yang, B.; Xiong, S.; Chen, C. Manipulation of Polymer Branching Density in Phosphine-Sulfonate Palladium and Nickel Catalyzed Ethylene Polymerization. *Polym. Chem.* **2017**, *8*, 6272–6276. (t) Zhang, D.; Chen, C. Influence

of Polyethylene Glycol Unit on Palladium- and Nickel-Catalyzed Ethylene Polymerization and Copolymerization. *Angew. Chem., Int. Ed.* **2017**, *56*, 14672–14676. (u) Song, G.; Pang, W.; Li, W.; Chen, M.; Chen, C. Phosphine-Sulfonate-Based Nickel Catalysts: Ethylene Polymerization and Copolymerization with Polar-Functionalized Norbornenes. *Polym. Chem.* **2017**, *8*, 7400–7405.

(4) (a) Nakano, R.; Chung, L. W.; Watanabe, Y.; Okuno, Y.; Okumura, Y.; Ito, S.; Morokuma, K.; Nozaki, K. Elucidating the Key Role of Phosphine–Sulfonate Ligands in Palladium-Catalyzed Ethylene Polymerization: Effect of Ligand Structure on the Molecular Weight and Linearity of Polyethylene. *ACS Catal.* **2016**, *6*, 6101–6113. (b) Noda, S.; Nakamura, A.; Kochi, T.; Chung, L. W.; Morokuma, K.; Nozaki, K. Mechanistic Studies on the Formation of Linear Polyethylene Chain Catalyzed by Palladium Phosphine-Sulfonate Complexes: Experiment and Theoretical Studies. *J. Am. Chem. Soc.* **2009**, *131*, 14088–14100.

(5) For bisphosphine monoxide (BPMO) and their related ligand systems, see: (a) Brassat, I.; Keim, W.; Killat, S.; Möhrath, M.; Mastroianni, P.; Nobile, C. F.; Suranna, G. P. Synthesis and Catalytic Activity of Allyl, Methallyl and Methyl Complexes of Nickel(II) and Palladium(II) with Biphosphine Monoxide Ligands: Oligomerization of Ethylene and Copolymerization of Ethylene and Carbon Monoxide. *J. Mol. Catal. A: Chem.* **2000**, *157*, 41–58. (b) Reisinger, C. M.; Nowack, R. J.; Volkmer, D.; Rieger, B. Novel Palladium Complexes Employing Mixed Phosphine Phosphonates and Phosphine Phosphinates as Anionic Chelating [P,O] Ligands. *Dalton Trans.* **2007**, 272–278. (c) Carrow, B. P.; Nozaki, K. Synthesis of Functional Polyolefins Using Cationic Bisphosphine Monoxide-Palladium Complexes. *J. Am. Chem. Soc.* **2012**, *134*, 8802–8805. (d) Contrella, N. D.; Sampson, J. R.; Jordan, R. F. Copolymerization of Ethylene and Methyl Acrylate by Cationic Palladium Catalysts That Contain Phosphine-Diethyl Phosphonate Ancillary Ligands. *Organometallics* **2014**, *33*, 3546–3555. (e) Sui, X.; Dai, S.; Chen, C. Ethylene Polymerization and Copolymerization with Polar Monomers by Cationic Phosphine Phosphonic Amide Palladium Complexes. *ACS Catal.* **2015**, *5*, 5932–5937. (f) Mitsushige, Y.; Carrow, B. P.; Ito, S.; Nozaki, K. Ligand-Controlled Insertion Regioselectivity Accelerates Copolymerisation of Ethylene with Methyl Acrylate by Cationic Bisphosphine Monoxide–Palladium Catalysts. *Chem. Sci.* **2016**, *7*, 737–744. (g) Johnson, A. M.; Contrella, N. D.; Sampson, J. R.; Zheng, M.; Jordan, R. F. Allosteric Effects in Ethylene Polymerization Catalysis. Enhancement of Performance of Phosphine-Phosphinate and Phosphine-Phosphonate Palladium Alkyl Catalysts by Remote Binding of $B(C_6F_5)_3$. *Organometallics* **2017**, *36*, 4990–5002. (h) Mitsushige, Y.; Yasuda, H.; Carrow, B. P.; Ito, S.; Kobayashi, M.; Tayano, T.; Watanabe, Y.; Okuno, Y.; Hayashi, S.; Kuroda, J.; Okumura, Y.; Nozaki, K. Methylene-Bridged Bisphosphine Monoxide Ligands for Palladium-Catalyzed Copolymerization of Ethylene and Polar Monomers. *ACS Macro Lett.* **2018**, *7*, 305–311. (i) Chen, M.; Chen, C. A Versatile Ligand Platform for Palladium- and Nickel-Catalyzed Ethylene Copolymerization with Polar Monomers. *Angew. Chem., Int. Ed.* **2018**, *57*, 3094–3098. (j) Zhang, W.; Waddell, P. M.; Tiedemann, M. A.; Padilla, C. E.; Mei, J.; Chen, L.; Carrow, B. P. B. P. Electron-Rich Metal Cations Enable Synthesis of High Molecular Weight, Linear Functional Polyethylenes. *J. Am. Chem. Soc.*, in press, DOI: 10.1021/jacs.8b04712.

(6) For phosphine–arenolate and their related ligand systems, see: (a) Xin, B. S.; Sato, N.; Tanna, A.; Oishi, Y.; Konishi, Y.; Shimizu, F. Nickel Catalyzed Copolymerization of Ethylene and Alkyl Acrylates. *J. Am. Chem. Soc.* **2017**, *139*, 3611–3614. (b) Konishi, Y.; Tao, W.; Yasuda, H.; Ito, S.; Oishi, Y.; Ohtaki, H.; Tanna, A.; Tayano, T.; Nozaki, K. Nickel-Catalyzed Propylene/Polar Monomer Copolymerization. *ACS Macro Lett.* **2018**, *7*, 213–217. (c) Zhang, Y.; Mu, H.; Pan, L.; Wang, X.; Li, Y. Robust Bulky [P,O] Neutral Nickel Catalysts for Copolymerization of Ethylene with Polar Vinyl Monomers. *ACS Catal.* **2018**, *8*, 5963–5976.

(7) For other ligand systems, see: (a) Britovsek, G. J. P.; Keim, W.; Mecking, S.; Sainz, D.; Wagner, T. Hemilabile P,O-Ligands in Palladium Catalyzed C–C Linkages: Codimerization of Ethylene and

- Styrene and Cooligomerization of Ethylene and Carbon Monoxide. *J. Chem. Soc., Chem. Commun.* **1993**, 1632–1634. (b) Mecking, S.; Keim, W. Cationic Palladium η^3 -Allyl Complexes with Hemilabile P,O-Ligands: Synthesis and Reactivity. Insertion of Ethylene into the Pd-Allyl Function. *Organometallics* **1996**, *15*, 2650–2656. (c) Liu, W.; Malinoski, J. M.; Brookhart, M. Ethylene Polymerization and Ethylene/Methyl 10-Undecenoate Copolymerization Using Nickel(II) and Palladium(II) Complexes Derived from a Bulky P,O Chelating Ligand. *Organometallics* **2002**, *21*, 2836–2838. (d) Malinoski, J. M.; Brookhart, M. Polymerization and Oligomerization of Ethylene by Cationic Nickel (II) and Palladium(II) Complexes Containing Bidentate Phenacyldiarylphosphine Ligands. *Organometallics* **2003**, *22*, 5324–5335. (e) Gott, A. L.; Piers, W. E.; Dutton, J. L.; McDonald, R.; Parvez, M. Dimerization of Ethylene by Palladium Complexes Containing Bidentate Trifluoroborate-Functionalized Phosphine Ligands. *Organometallics* **2011**, *30*, 4236–4249. (f) Kim, Y.; Jordan, R. F. Synthesis, Structures, and Ethylene Dimerization Reactivity of Palladium Alkyl Complexes That Contain a Chelating Phosphine-Trifluoroborate Ligand. *Organometallics* **2011**, *30*, 4250–4256. (g) Zhang, Y.; Cao, Y.; Leng, X.; Chen, C.; Huang, Z. Cationic Palladium(II) Complexes of Phosphine–Sulfonamide Ligands: Synthesis, Characterization, and Catalytic Ethylene Oligomerization. *Organometallics* **2014**, *33*, 3738–3745.
- (8) For group 10 metal complexes that bear a bidentate ligand with an NHC moiety, see: (a) Waltman, A. W.; Grubbs, R. H. A New Class of Chelating N-Heterocyclic Carbene Ligands and Their Complexes with Palladium. *Organometallics* **2004**, *23*, 3105–3107. (b) Ketz, B. E.; Ottenwaelder, X. G.; Waymouth, R. M. Synthesis, Structure, and Olefin Polymerization with Nickel(II) N-Heterocyclic Carbene Enolates. *Chem. Commun.* **2005**, 848, 5693–5695. (c) Nagai, Y.; Kochi, T.; Nozaki, K. Synthesis of N-Heterocyclic Carbene-Sulfonate Palladium Complexes. *Organometallics* **2009**, *28*, 6131–6134. (d) Zhou, X.; Jordan, R. F. Cis/Trans Isomerization, and Reactivity of Palladium Alkyl Complexes That Contain a Chelating N-Heterocyclic-Carbene Sulfonate Ligand. *Organometallics* **2011**, *30*, 4632–4642. (e) Khllebnikov, V.; Meduri, A.; Mueller-Bunz, H.; Montini, T.; Fornasiero, P.; Zangrando, E.; Milani, B.; Albrecht, M. Palladium Carbene Complexes for Selective Alkene Di- and Oligomerization. *Organometallics* **2012**, *31*, 976–986. (f) Tao, W.; Akita, S.; Nakano, R.; Ito, S.; Hoshimoto, Y.; Ogoshi, S.; Nozaki, K. Copolymerisation of Ethylene with Polar Monomers by Using Palladium Catalysts Bearing an N-Heterocyclic Carbene–phosphine Oxide Bidentate Ligand. *Chem. Commun.* **2017**, 53, 2630–2633.
- (9) (a) Nakano, R.; Nozaki, K. Copolymerization of Propylene and Polar Monomers Using Pd/IzQO Catalysts. *J. Am. Chem. Soc.* **2015**, *137*, 10934–10937. (b) Tao, W.; Nakano, R.; Ito, S.; Nozaki, K. Copolymerization of Ethylene and Polar Monomers by Using Ni/IzQO Catalysts. *Angew. Chem., Int. Ed.* **2016**, *55*, 2835–2839. (c) Yasuda, H.; Nakano, R.; Ito, S.; Nozaki, K. Palladium/IzQO-Catalyzed Coordination–Insertion Copolymerization of Ethylene and 1,1-Disubstituted Ethylenes Bearing a Polar Functional Group. *J. Am. Chem. Soc.* **2018**, *140*, 1876–1883.
- (10) (a) Fantasia, S.; Petersen, J. L.; Jacobsen, H.; Cavallo, L.; Nolan, S. P. Electronic Properties of N-Heterocyclic Carbene (NHC) Ligands: Synthetic, Structural, and Spectroscopic Studies of (NHC)-Platinum(II) Complexes. *Organometallics* **2007**, *26*, 5880–5889. (b) Nelson, D. J.; Nolan, S. P. Quantifying and Understanding the Electronic Properties of N-Heterocyclic Carbenes. *Chem. Soc. Rev.* **2013**, *42*, 6723–6753.
- (11) For the synthesis of the imine, see: Hu, P.; Qiao, Y.-L.; Wang, J.-Q.; Jin, G.-X. Syntheses, Characterization, and Ethylene Polymerization of Titanium Complexes with Double-Duty Tridentate [ONN] Ligands. *Organometallics* **2012**, *31*, 3241–3247.
- (12) For reviews on ligand substitution, see: (a) Anderson, G. K.; Cross, R. J. Isomerisation Mechanisms of Square-Planar Complexes. *Chem. Soc. Rev.* **1980**, *9*, 185–215. (b) Cross, R. J. Ligand Substitution Reactions of Square-Planar Molecules. *Chem. Soc. Rev.* **1985**, *14*, 197–223.
- (13) For the crystal structure of a pyridine complex, see: (a) Newsham, D. K.; Borkar, S.; Sen, A.; Conner, D. M.; Goodall, B. L. Inhibitory Role of Carbon Monoxide in Palladium(II)-Catalyzed Nonalternating Ethene/Carbon Monoxide Copolymerizations and the Synthesis of Polyethylene-Block-Poly(Ethene-Alt-Carbon Monoxide). *Organometallics* **2007**, *26*, 3636–3638. For the crystal structure of a 2,6-lutidine complex, see: (b) Kochi, T.; Noda, S.; Yoshimura, K.; Nozaki, K. *J. Am. Chem. Soc.* **2007**, *129*, 8948–8949.
- (14) (a) Mecking, S.; Johnson, L. K.; Wang, L.; Brookhart, M. Mechanistic Studies of the Palladium-Catalyzed Copolymerization of Ethylene and α -Olefins with Methyl Acrylate. *J. Am. Chem. Soc.* **1998**, *120*, 888–899. (b) Dai, S.; Zhou, S.; Zhang, W.; Chen, C. Systematic Investigations of Ligand Steric Effects on α -Diimine Palladium Catalyzed Olefin Polymerization and Copolymerization. *Macromolecules* **2016**, *49*, 8855–8862.
- (15) (a) Lee, C.; Yang, W.; Parr, R. G. Development of the Colle-Salvetti Correlation-Energy Formula into a Functional of the Electron Density. *Phys. Rev. B* **1988**, *37*, 785–789. (b) Miehlich, B.; Savin, A.; Stoll, H.; Preuss, H. Results Obtained with the Correlation Energy Density Functionals of Becke and Lee, Yang and Parr. *Chem. Phys. Lett.* **1989**, *157*, 200–206. (c) Becke, A. D. Density-Functional Thermochemistry. III. The Role of Exact Exchange. *J. Chem. Phys.* **1993**, *98*, 5648–5652.
- (16) Grimme, S.; Antony, J.; Ehrlich, S.; Krieg, H. A Consistent and Accurate Ab Initio Parametrization of Density Functional Dispersion Correction (DFT-D) for the 94 Elements H–Pu. *J. Chem. Phys.* **2010**, *132*, 154104.
- (17) Hay, P. J.; Wadt, W. R. Ab Initio Effective Core Potentials for Molecular Calculations. Potentials for the Transition Metal Atoms Sc to Hg. *J. Chem. Phys.* **1985**, *82*, 270–283.
- (18) (a) Ditchfield, R.; Hehre, W. J.; Pople, J. A. Self-Consistent Molecular-Orbital Methods. IX. An Extended Gaussian-Type Basis for Molecular-Orbital Studies of Organic Molecules. *J. Chem. Phys.* **1971**, *54*, 724–728. (b) Hehre, W. J.; Ditchfield, R.; Pople, J. A. Self-Consistent Molecular Orbital Methods. XII. Further Extensions of Gaussian-Type Basis Sets for Use in Molecular Orbital Studies of Organic Molecules. *J. Chem. Phys.* **1972**, *56*, 2257–2261.
- (19) Marenich, A. V.; Cramer, C. J.; Truhlar, D. G. Universal Solvation Model Based on Solute Electron Density and a Continuum Model of the Solvent Defined by the Bulk Dielectric Constant and Atomic Surface Tensions. *J. Phys. Chem. B* **2009**, *113*, 6378–6396.
- (20) Sato, Y.; Hosaka, N.; Inomata, H.; Kanaka, K. Solubility of Ethylene in Toluene, Norbornene, and Toluene+norbornene Mixture. *Fluid Phase Equilib.* **2013**, *344*, 112–116.
- (21) (a) Back, O.; Henry-Ellinger, M.; Martin, C. D.; Martin, D.; Bertrand, G. ^{31}P NMR Chemical Shifts of Carbene–Phosphinidene Adducts as an Indicator of the π -Accepting Properties of Carbenes. *Angew. Chem., Int. Ed.* **2013**, *52*, 2939–2943. (b) Verlinden, K.; Buhl, H.; Frank, W.; Ganter, C. Determining the Ligand Properties of N-Heterocyclic Carbenes from ^{77}Se NMR Parameters. *Eur. J. Inorg. Chem.* **2015**, 2416–2425. For the energy values of the vacant p-orbitals, see Section 6 in the Supporting Information.
- (22) For reviews on cis/trans isomerization, see ref 12.
- (23) Zhou, X.; Lau, K.; Petro, B. J.; Jordan, R. F. cis/trans Isomerization of *o*-Phosphino-Arenesulfonate Palladium Methyl Complexes. *Organometallics* **2014**, *33*, 7209–7214.
- (24) Zheng, F.; Hutton, A. T.; van Sittert, C. G. C. E.; Moss, J. R.; Mapolie, S. F. Synthesis, structural characterization and cis–trans isomerization of novel (salicylaldiminato)platinum(II) complexes. *Dalton Trans.* **2013**, 42, 11163–11179.
- (25) cis-5-Lut exists in equilibrium with the dimeric species meso- and rac-(cis-5) $_2$, which were also observed by ^1H NMR analysis in a solution of cis-5-Lut. When an excess amount of 2,6-lutidine was added to the solution containing (cis-5) $_2$ and cis-5-Lut, (cis-5) $_2$ reacted with 2,6-lutidine to form cis-5-Lut. For details, see Section 2 in the Supporting Information.
- (26) Frisch, M. J.; Trucks, G. W.; Schlegel, H. B.; Scuseria, G. E.; Robb, M. A.; Cheeseman, J. R.; Scalmani, G.; Barone, V.; Mennucci, B.; Petersson, G. A.; Nakatsuji, H.; Caricato, M.; Li, X.; Hratchian, H.

P.; Izmaylov, A. F.; Bloino, J.; Zheng, G.; Sonnenberg, J. L.; Hada, M.; Ehara, M.; Toyota, K.; Fukuda, R.; Hasegawa, J.; Ishida, M.; Nakajima, T.; Honda, Y.; Kitao, O.; Nakai, H.; Vreven, T.; Montgomery, J. A., Jr.; Peralta, J. E.; Ogliaro, F.; Bearpark, M.; Heyd, J. J.; Brothers, E.; Kudin, K. N.; Staroverov, V. N.; Keith, T.; Kobayashi, R.; Normand, J.; Raghavachari, K.; Rendell, A.; Burant, J. C.; Iyengar, S. S.; Tomasi, J.; Cossi, M.; Rega, N.; Millam, M. J.; Klene, M.; Knox, J. E.; Cross, J. B.; Bakken, V.; Adamo, C.; Jaramillo, J.; Gomperts, R.; Stratmann, R. E.; Yazyev, O.; Austin, A. J.; Cammi, R.; Pomelli, C.; Ochterski, J. W.; Martin, R. L.; Morokuma, K.; Zakrzewski, V. G.; Voth, G. A.; Salvador, P.; Dannenberg, J. J.; Dapprich, S.; Daniels, A. D.; Farkas, Ö.; Foresman, J. B.; Ortiz, J. V.; Cioslowski, J.; Fox, D. J. *Gaussian 09*, Revision D.01; Gaussian, Inc.: Wallingford, CT, 2013.